Inorg. Chem. **1998,** *37,* 3779−3784 **3779**

Kinetic Study on the Substitution of Dimethylacetamide for the Terminal Aqua Ligands in the Trinuclear Chromium(III) Complexes $[Cr_3(\mu_3\text{-}O)(\mu\text{-}RCO_2)_6(H_2O)_3]^+$ (R = H, CH_3, CH_3CH_2, CH_2Cl, $CHCl_2$, CH_3OCH_2, $(CH_3)_3C$, CH_2ClCH_2, $(CH_3CH_2)_2CH$). Elucidation of the Mechanism from the Activation Volumes and the Substituent Effects of Bridging Carboxylate Ligands

Takashi Fujihara,*,† Jun Aonahata,† Shigekazu Kumakura,† Akira Nagasawa,*,†
Kazuhiro Murakami,‡ and Tasuku Ito§

Department of Chemistry, Faculty of Science, Saitama University, Urawa, Saitama 338-8570, Japan, Department of Chemistry, Faculty of Science, Tohoku University, Aramaki, Aoba-ku, Sendai 980-8578, Japan, and Department of Chemistry, Graduate School of Science, Tohoku University, Aramaki, Aoba-ku, Sendai 980-8578, Japan

Received January 2, 1998

The substitution of dimethylacetamide (dma) for the terminal aqua ligands in the carboxylate-bridged trinuclear chromium(III) complex $[Cr_3(\mu_3\text{-}O)(\mu\text{-}RCO_2)_6(H_2O)_3]^+$ (R = H, CH_3, CH_3CH_2, CH_2Cl, $CHCl_2$, CH_3OCH_2, $(CH_3)_3C$, CH_2ClCH_2, $(CH_3CH_2)_2CH$) in dma was kinetically studied by UV−visible absorption at 25−50 °C and 0.1−232 MPa. The time course is uniphasic over all three steps of the ligand replacement. The substitution rate k varied from $2.4(1) \times 10^{-5}$ (R = $CHCl_2$) to $9.49(2) \times 10^{-3}$ (R = $C(CH_3)_3$) s^{-1} depending on the substituent R at 40 °C. Large positive activation parameters $\Delta H^‡$ (98−123 kJ mol^{-1}), $\Delta S^‡$ (29−81 J K^{-1} mol^{-1}), and $\Delta V^‡$ (12.4−21.3 cm^3 mol^{-1}) for all the complexes suggested a dissociative activation mode (D or I_d mechanism). It is similar to those for terminal ligand substitution of acetate-bridged trinuclear complexes of ruthenium(III) and rhodium(III) with a μ_3-O ligand and molybdenum with two μ_3-O ligands. Examination of the substituent effect disclosed a linear relationship between k and Taft's electronic parameters, as well as pK_a (RCOOH), indicating that the σ-donor ability of the bridging carboxylate affects the strength of the $Cr-OH_2$ bond in the cis position. The crystals of $[Cr_3(\mu_3\text{-}O)(\mu\text{-}RCO_2)_6(H_2O)_3][B(C_6H_5)_4]\cdot nH_2O$ (R = H (**1b**), $n = 6$; R = CH_3 (**2b**), $n = 2$) were found to be triclinic with space group $P\bar{1}$, $a = 9.2080(8)$ Å, $b = 14.724(2)$ Å, and $c = 15.308(2)$ Å, $\alpha = 79.369(6)°$, $\beta = 86.513(8)°$, $\gamma = 79.823(8)°$, $Z = 2$, and $V = 2006.5(4)$ Å^3 and with space group $P\bar{1}$, $a = 8.848(6)$ Å, $b = 15.057(7)$ Å, $c = 17.375(8)$ Å, $\alpha = 107.82(3)°$, $\beta = 104.57(4)°$, $\gamma = 92.27(4)°$, $Z = 2$, and $V = 2116(2)$ Å^3, respectively. The relatively longer $Cr-OH_2$ distances (average 2.03(1) and 2.06(2) Å for **1b** and **2b**, respectively) than those of the mononuclear chromium(III) aqua complexes, due to a trans effect of the central oxide ion and the additional cis effect of the bridging carboxylate, play a role in accelerating the dissociative substitution for the terminal ligands.

Introduction

A number of (μ_3-oxo)hexakis(μ-carboxylato)tris(unidentate)-trimetal(III) ions, $[M_3(\mu_3\text{-}O)(\mu\text{-}RCO_2)_6(L)_3]^+$ (L = H_2O, pyridine (py) and its derivatives), have been investigated from structural, magnetic, electrochemical, and kinetic points of view.[1−24] We have studied the kinetics of the aqua ligand substitution in a series of ruthenium and rhodium complexes, $[M_3(\mu_3\text{-}O)(\mu\text{-}CH_3CO_2)_6(H_2O)_3]^+$ (M_3 = Ru_3, Rh_3, Ru_2Rh), in

---

† Saitama University.
‡ Faculty of Science, Tohoku University.
§ Graduate School of Science, Tohoku University.

(1) Bourke, J. P.; Karu, E.; Cannon, R. D. *Inorg. Chem.* **1996**, *35*, 1557.
(2) Anson, C. E.; Bourke, J. P.; Cannon, R. D.; Jayasooriya, U. A.; Molinier, M.; Powell, A. K. *Inorg. Chem.* **1997**, *36*, 1265.
(3) Glowiak, T.; Kozlowsk, H.; Erre, L. S.; Micera, G. *Inorg. Chim. Acta* **1996**, *248*, 99.
(4) Harton, A.; Nagi, M. K.; Glass, M. M.; Junk, P. C.; Atwood, J. L.; Vincent, J. B. *Inorg. Chim. Acta* **1994**, *217*, 171.
(5) Belmore, K.; Madison, X. J.; Harton, A.; Vincent, J. B. *Spectrochim. Acta* **1994**, *50A*, 2365.
(6) Sasaki, Y.; Nagasawa, A.; Tokiwa-Yamamoto, A.; Ito, T. *Inorg. Chim. Acta* **1993**, *212*, 175.
(7) Glass, M. M.; Belmore, K.; Vincent, J. B. *Polyhedron* **1993**, *12*, 133.
(8) Anson, C. E.; Chai-Sa'aed, N.; Bourke, J. P.; Cannon, R. D.; Jayasooriya, U. A.; Powell, A. K. *Inorg. Chem.* **1993**, *32*, 1502.
(9) Mullica, D. F.; Pennington, D. E.; Bradshaw, J. E.; Sappenfield, E. L. *Inorg. Chim.* Acta **1992**, *191*, 3.
(10) Andras, M. T.; Duraj, S. A.; Hepp, A. F.; Fanwick, P. E.; Bodnar, M. M. *J. Am. Chem.* Soc. **1992**, *114*, 786.
(11) Kato, H.; Nakata, K.; Nagasawa, A.; Yamaguchi, T.; Sasaki, Y.; Ito, T. *Bull. Chem. Soc. Jpn.* **1991**, *64*, 3463.
(12) (a) Nakata, K.; Nagasawa, A.; Sasaki, Y.; Ito, T. *Chem. Lett.* **1989**, 753. (b) Nakata, K.; Nagasawa, A.; Soyama, N.; Sasaki, Y.; Ito, T. *Inorg. Chem.* **1991**, *30*, 1575.
(13) Jayasooriya, U. A.; Cannon, R. D.; White, R. P.; Kearley, G. J. *Angew. Chem., Int. Ed. Engl.* **1989**, *28*, 930.
(14) Cannon, R. D.; White, R. P. *Prog. Inorg. Chem.* **1988**, *36*, 195−298.
(15) Summer, C. E., Jr. *Inorg. Chem.* **1988**, *27*, 1320.
(16) Sasaki, Y.; Tokiwa, A.; Ito, T. *J. Am. Chem. Soc.* **1987**, *109*, 6341.
(17) Hills, E. F.; Richens, D. T.; Sykes, A. G. *Inorg. Chem.* **1986**, *25*, 3144.
(18) Gonzalez-Vergara, E.; Hegenauer, J.; Saltman, P.; Sabat, M.; Ibers, J. A. *Inorg. Chim. Acta* **1982**, *66*, 115.
(19) Johnson, M. K.; Powell, D. B.; Cannon, R. D. *Spectrochim. Acta* **1981**, *37A*, 995.
(20) Uemura, S.; Spencer, A.; Wilkinson, G. *J. Chem. Soc., Dalton Trans.* **1973**, 2565.

S0020-1669(98)00001-9 CCC: $15.00

CD_3OD by ^1H NMR, and disclosed a remarkable labilization, as compared with the case of mononuclear complexes of these metal ions, and the intramolecular interactive effect of mixing different metal ions.[6] The trans effect of the central oxide ion was considered as a major factor responsible for the labilization. A dissociative mechanism was proposed for all those reactions on the basis of the activation parameters. There have been few studies, however, on the substitution reactions of the trinuclear chromium(III) "basic carboxylate" complexes. Recently, Bourke, Karu, and Cannon studied the kinetics of the formation and dissociation of $[Cr_3(\mu_3\text{-}O)(\mu\text{-}CH_3CO_2)_6(urea)_3]^+$.[1]

We report here the syntheses and the kinetics of the substitution of dimethylacetamide (dma) for the terminal aqua ligands for the nine aliphatic carboxylate-bridged trinuclear chromium(III) complexes $[Cr_3(\mu_3\text{-}O)(\mu\text{-}RCO_2)_6(H_2O)_3]^+$ (R = H (**1**), CH_3 (**2**), CH_3CH_2 (**3**), CH_2Cl (**4**), $CHCl_2$ (**5**), CH_3OCH_2 (**6**), $(CH_3)_3C$ (**7**), CH_2ClCH_2 (**8**), $(CH_3CH_2)_2CH$ (**9**)) at various temperatures under atmospheric and elevated pressures in connection with their structures. The rates of substitution in the trinuclear chromium(III) complexes in relation to the molecular structures will be discussed to reveal the effects of the mutual ligand such as the central oxo ion and the bridging carboxylates.

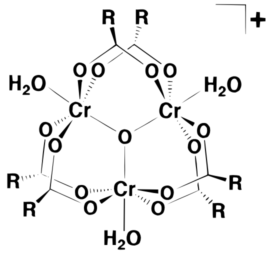

1–9

Experimental Section

Materials. Dried and distilled dimethylacetamide (dma) was employed routinely. The following deuterated chemicals were used as received: acetic acid-d_4 (CD_3CO_2D, 99% deuterated) and D_2O from Aldrich; formic acid-d_2 (DCO_2D, 99% deuterated) from ISOTEC Inc. All other chemicals were used without further purification.

Preparation of Complexes. $[Cr_3(\mu_3\text{-}O)(\mu\text{-}RCO_2)_6(H_2O)_3]NO_3$ (R = H (1a), CH_3 (2a), CH_3CH_2 (3a), CH_2Cl (4), $CHCl_2$ (5), CH_3OCH_2 (6), $(CH_3)_3C$ (7), CH_2ClCH_2 (8), $(CH_3CH_2)_2CH$ (9)). All the complexes were synthesized by the following method. $Cr(NO_3)_3\cdot 9H_2O$ (8 g, 20 mmol) and an appropriate carboxylic acid (40 mmol) were dissolved in acetone (100 cm^3), and the mixture was refluxed for 5 h and filtered at room temperature. To the green filtrate concentrated to ca. 30 cm^3 under reduced pressure were/was added chloroform and/or diethyl ether to obtain green solids, which were then filtered off and washed with chloroform and diethyl ether successively. The recrystallization was accomplished from acetone/chloroform. Anal. Found (calcd) for **1a:** C, 13.01 (12.91); H, 2.22 (2.17); N, 1.48 (2.51). Yield (based on Cr): 85%. Anal. Found (calcd) for **2a**$\cdot 3H_2O$: C, 20.55 (20.70); H, 4.25 (4.34); N, 1.98 (2.01). Yield: 90%. Anal. Found (calcd) for **3a**$\cdot 2H_2O$: C, 28.55 (28.35); H, 5.20 (5.29); N, 1.87 (1.84). Yield: 75%. Anal. Found (calcd) for **4**$\cdot 3H_2O$: C, 16.02 (15.96); H, 2.61 (2.68); N, 1.57 (1.55). Yield: 85%. Anal. Found (calcd) for **5**$\cdot H_2O$: C, 13.09 (13.42); H, 1.31 (1.31); N, 1.32 (1.30). Yield: 70%. Anal. Found (calcd) for **6**: C, 25.12 (26.29); H, 4.37 (4.41); N, 1.70 (1.70). Yield: 95%. Anal. Found (calcd) for **7**$\cdot H_2O$: C, 40.05 (39.48); H, 6.91 (6.85); N, 1.55 (1.53). Yield: 80%. Anal. Found (calcd) for **8**$\cdot 2H_2O$: C, 22.29 (22.31); H, 3.50 (3.54); N, 1.48(1.45). Yield: 85%.

$[Cr_3(\mu_3\text{-}O)(\mu\text{-}RCO_2)_6(H_2O)_3][B(C_6H_5)_4]\cdot nH_2O$ (R = H (1b), CH_3 (2b), CH_3CH_2 (3b)). To an aqueous solution (20 cm^3) of $[Cr_3(\mu_3\text{-}O)(\mu\text{-}RCO_2)_6(H_2O)_3]NO_3\cdot nH_2O$ (R = H, CH_3, CH_3CH_2) (7 mmol) was added 20 cm^3 of an aqueous solution of $NaB(C_6H_5)_4$ (4.0 g, 12 mmol) with stirring, the mixture was filtered, and the filtrate was set aside in a refrigerator for 3 h. Green crystals were filtered off, washed with ice-cooled water, and dried in vacuo. Anal. Found (calcd) for **1b**$\cdot 6H_2O$: C, 39.21 (39.02); H, 4.75 (4.80). Yield: 45%. Anal. Found (calcd) for **2b**$\cdot 2H_2O$: C, 46.42 (46.22); H, 5.15 (5.17). Yield: 50%. Anal. Found (calcd) for **3b**$\cdot 2H_2O$: C, 52.42 (51.28); H, 5.80 (5.74). Yield: 55%.

$[Cr_3(\mu_3\text{-}O)(\mu\text{-}RCO_2)_6(dma)_3]NO_3$. $[Cr_3(\mu_3\text{-}O)(\mu\text{-}RCO_2)_6(H_2O)_3]NO_3$ (7 mmol) was dissolved in dma (50 cm^3) with stirring; the mixture was heated for 4 h at 100 °C and then evaporated to dryness under reduced pressure at 40 °C. The green residue was dissolved in dma and reprecipitated by adding diethyl ether. Ultraviolet−visible absorption (UV−vis) spectra of the precipitates were very similar in the pattern to those of the reaction mixture after digestion, although analytical results indicated that the solid was a mixture with partly substituted complexes.

Deuterated Complexes. The complexes with $\mu\text{-}CD_3CO_2^-$ and $\mu\text{-}DCO_2^-$ as bridging carboxylates and D_2O as terminal ligands were prepared by the same procedure as noted above using CD_3CO_2D, DCO_2D, and D_2O in place of the nondeuterated ligands.

Measurements. UV−vis spectra were recorded on a JASCO V-560 or a Shimadzu UV-160 spectrophotometer at room temperature. Hydrogen-2 (^2H) NMR spectra were obtained using a Bruker ARX 400 FT-NMR spectrometer at 25 °C under the following conditions: concentration of the complex, ca. 5×10^{-3} M; sample tube diameter, 10 mm; external standard, $CDCl_3$ (δ 7.24). The temperature-dependent magnetic susceptibility of powder samples were collected on a Quantum Design Model MPMS SQUID-based magnetometer at 5−300 K. The corrected susceptibility χ after subtracting the diamagnetic influence was provided for a nonlinear least-squares fit of χ vs T, and an isotropic spin exchange coupling constant J (in cm^{-1}) was derived with the Van Vleck equation defined by the exchange Hamiltonian $H = -2J\sum(S_i\cdot S_j)$.

Kinetic Measurements. The substitutions of dma for the terminal aqua ligands were monitored by the increase in UV−vis absorptions at 600 nm. Each complex was dissolved quickly in dma (ca. 3×10^{-3} M) at room temperature, and the solution was poured into a 10 mm quartz cell at a given temperature in a JASCO V-560 spectrophotometer with a variable-cell-temperature controller. Pseudo-first-order rate relationships were obtained by following the reactions for at least 4 half-lives, and the rate constants (k_{obs}) were determined by nonlinear least-squares fits for the following relationship:

$$A_t = A_{inf} + (A_0 - A_{inf}) \exp(-k_{obs}t) \qquad (1)$$

where A_0, A_{inf}, and A_t refer to the absorbances at the initial time, infinite time, and time t, respectively (see Figure S2, Supporting Information). At least three kinetic runs were carried out for each aliquot.

The reactions under elevated pressures were carried out as follows. A solution of the complex (ca. 3×10^{-3} M) in dma prepared at 0 °C was sealed in a optical cell, which consisted of a quartz pipe (1.0-cm inner diameter and 2.0-cm length) and two Teflon stopping pistons with silicon rubber O-rings at the top and the bottom. The cell was placed in a high-pressure vessel, a stainless steel block with optical sapphire windows, from Hikari High-Pressure Machinery (Hiroshima, Japan), and locked with a stainless steel screw cap. The vessel was set on a light path in a spectrophotometer, and the pressure was applied through thermostated methanol inside with a hand pump. A Bourdon tube calibrated with a Heise standard gauge was used for the pressure measurements (18.0, 41.8, 89.4, 185, and 232 MPa (±0.5 MPa)).

Crystal Structure Determinations. Crystal data for **1b**$\cdot 6H_2O$: $M = 923.45$, triclinic, space group $P\bar{1}$, $a = 9.2080(8)$ Å, $b = 14.724(2)$ Å, $c = 15.308(2)$ Å, $\alpha = 79.369(6)°$, $\beta = 86.513(8)°$, $\gamma = 79.823(8)°$, $Z = 2$, $V = 2006.5(4)$ Å^3, $D_c = 1.497$ g cm^{-3}, green crystal 0.2 × 0.2 × 0.1 mm, μ(Mo Kα) = 8.543 cm^{-1}. Crystal data for **2b**$\cdot 2H_2O$: $M =$

---

(21) Ferguson, J.; Güdel, H. U. *Chem. Phys. Lett.* **1972**, *17*, 547.
(22) Chang, S. C.; Jeffrey, G. A. *Acta Crystallogr.* **1970**, *B26*, 673.
(23) Dubicki, L.; Martin, R. L. *Aust. J. Chem.* **1969**, *22*, 701.
(24) Earnshaw, A.; Figgis, B. N.; Lewis, J. *J. Chem. Soc. A* **1966**, 1656.

Table 1. Selected Bond Lengths (Å) and Bond Angles (deg) for $\mathbf{1b}\cdot 6H_2O$ and $\mathbf{2b}\cdot 2H_2O$

$\mathbf{1b}\cdot 6H_2O$		$\mathbf{2b}\cdot 2H_2O$	
Cr(1)−O(1)	1.910(2)	Cr(1)−O(1)	1.892(1)
Cr(1)−O(2)	1.963(3)	Cr(1)−O(2)	1.960(2)
Cr(1)−O(4)	1.985(3)	Cr(1)−O(5)	1.959(2)
Cr(1)−O(6)	1.982(3)	Cr(1)−O(6)	1.983(2)
Cr(1)−O(8)	1.974(3)	Cr(1)−O(8)	1.973(2)
Cr(1)−O(14)	2.029(3)	Cr(1)−O(14)	2.084(1)
Cr(2)−O(1)	1.913(2)	Cr(2)−O(1)	1.895(1)
Cr(2)−O(3)	1.967(3)	Cr(2)−O(3)	1.972(2)
Cr(2)−O(5)	1.987(3)	Cr(2)−O(4)	1.967(2)
Cr(2)−O(11)	1.973(3)	Cr(2)−O(10)	1.964(2)
Cr(2)−O(13)	1.979(3)	Cr(2)−O(12)	1.963(2)
Cr(2)−O(15)	2.011(3)	Cr(2)−O(15)	2.069(2)
Cr(3)−O(1)	1.903(2)	Cr(3)−O(1)	1.886(1)
Cr(3)−O(7)	1.985(3)	Cr(3)−O(7)	1.987(2)
Cr(3)−O(9)	1.962(3)	Cr(3)−O(9)	1.963(2)
Cr(3)−O(10)	1.980(3)	Cr(3)−O(11)	1.965(2)
Cr(3)−O(12)	1.963(3)	Cr(3)−O(13)	1.995(2)
Cr(3)−O(16)	2.044(3)	Cr(3)−O(16)	2.040(2)
Cr(1)−Cr(2)	3.3142(6)	Cr(1)−Cr(2)	3.2829(2)
Cr(2)−Cr(3)	3.3018(6)	Cr(2)−Cr(3)	3.2802(3)
Cr(3)−Cr(1)	3.3027(6)	Cr(3)−Cr(1)	3.2635(2)
O(1)Cr(1)O(2)	95.7(1)	O(1)Cr(1)O(2)	96.1(1)
O(1)Cr(1)O(4)	94.0(1)	O(1)Cr(1)O(5)	93.1(1)
O(1)Cr(1)O(6)	94.3(1)	O(1)Cr(1)O(6)	94.5(1)
O(1)Cr(1)O(8)	95.2(1)	O(1)Cr(1)O(8)	97.0(1)
O(1)Cr(1)O(14)	178.9(1)	O(1)Cr(1)O(14)	177.8(1)
O(1)Cr(2)O(3)	94.7(1)	O(1)Cr(2)O(3)	96.1(1)
O(1)Cr(2)O(5)	94.2(1)	O(1)Cr(2)O(4)	93.1(1)
O(1)Cr(2)O(11)	94.4(1)	O(1)Cr(2)O(10)	94.5(1)
O(1)Cr(2)O(13)	94.6(1)	O(1)Cr(2)O(12)	97.0(1)
O(1)Cr(2)O(15)	179.0(1)	O(1)Cr(2)O(15)	177.8(1)
O(1)Cr(3)O(7)	93.5(1)	O(1)Cr(3)O(7)	94.6(1)
O(1)Cr(3)O(9)	95.7(1)	O(1)Cr(3)O(9)	95.3(1)
O(1)Cr(3)O(10)	95.4(1)	O(1)Cr(3)O(11)	93.8(1)
O(1)Cr(3)O(12)	96.4(1)	O(1)Cr(3)O(13)	96.2(1)
O(1)Cr(3)O(16)	177.7(1)	O(1)Cr(3)O(16)	179.4(1)
Cr(1)O(1)Cr(2)	120.2(1)	Cr(1)O(1)Cr(2)	120.2(1)
Cr(2)O(1)Cr(3)	119.8(1)	Cr(2)O(1)Cr(3)	120.3(1)
Cr(3)O(1)Cr(1)	120.0(1)	Cr(3)O(1)Cr(1)	119.5(1)

935.17, triclinic, space group $P\bar{1}$, $a = 8.848(6)$ Å, $b = 15.057(7)$ Å, $c = 17.375(8)$ Å, $\alpha = 107.82(3)°$, $\beta = 104.57(4)°$, $\gamma = 92.27(4)°$, $Z = 2$, $V = 2116(2)$ Å^3, $D_c = 1.468$ g cm^{-3}, green crystal 0.2 × 0.2 × 0.2 mm, μ(Mo Kα) = 8.079 cm^{-1}.

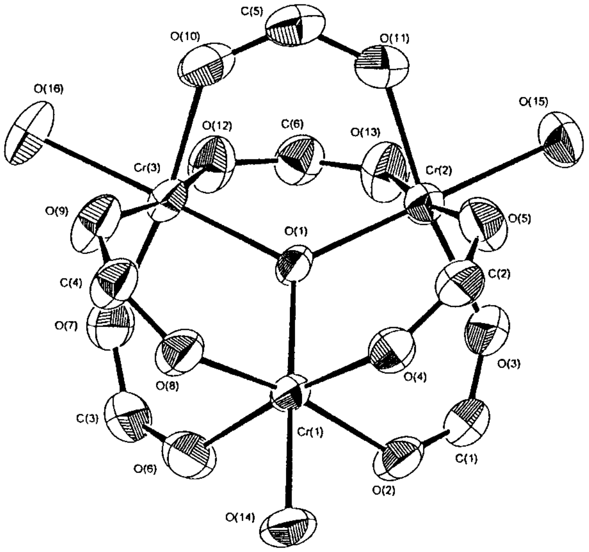

Figure 1. ORTEP drawing of the $[Cr_3(\mu_3\text{-}O)(\mu\text{-}HCO_2)_6(H_2O)_3]^+$ (**1**) cation in the crystals of the $[B(C_6H_5)_4]^-$ salt (**1b**) with the thermal ellipsoids drawn at the 50% probability level.

Crystals suitable for X-ray analysis of $\mathbf{1b}\cdot 6H_2O$ and $\mathbf{2b}\cdot 2H_2O$ were obtained by slow evaporation of the corresponding concentrated aqueous solutions. Weissenberg photographs were recorded on 30 frames of imaging plates mounted on a Mac Science DIP3000 diffractometer equipped with a rotating Mo anode (50 kV, 300 mA, $\lambda = 0.716\ 09$ Å) at room temperature, each of which was taken around the ω axis with a ocsillation range of 6°. Intensity data were collected using Mac Science XDIP software; the integration of reflection intensities and data reduction were carried out by DENZO software.[25] The unit cell were determined by the routine SCALEPACK[25] in DENZO employing all refections observed.

The structures were solved by direct methods (SIR 92[26]) and expanded using Fourier techniques. All non-hydrogen atoms were refined with anisotropic thermal parameters. Hydrogen atoms were not included in the calculation. The positional and thermal parameters were refined by full-matrix least-squares procedures. The final cycles of full-matrix least-squares refinements for $\mathbf{1b}\cdot 6H_2O$ and $\mathbf{2b}\cdot 2H_2O$ were based on the 5884 observed reflections and 505 variable parameters and on the 8243 observed reflections and 523 variable parameters, respectively. The final values of R, R_w for $\mathbf{1b}\cdot 6H_2O$ and $\mathbf{2b}\cdot 2H_2O$ were 0.064, 0.079 and 0.051, 0.068, respectively. Absorption and decay corrections were not applied. All calculations were performed using the Crystan-GM[27] crystallographic software package of Mac Science on a Sun Sparc 10 workstation at the Chemical Analysis Center, Saitama University.

Results and Discussion

Preparation of Complexes. Harton et al. have reported a one-pot synthesis of a benzoate-bridged trinuclear complex in ethanol or acetonitrile.[4] Results of our kinetic studies on Ru, Rh, Mo, and W trinuclear complexes[6,12,16] indicate that donor solvents such as EtOH and CH_3CN are not appropriate for synthetic procedures, since the substitution for terminal aqua ligands occurs easily. Preliminary experiments disclosed that UV−vis spectra of $[Cr_3(\mu_3\text{-}O)(\mu\text{-}CH_3CO_2)_6(H_2O)_3]^+$ (**2**) in EtOH and CH_3CN change with time, probably due to the substitution of the solvent molecule. We adopted, therefore, the less-donating media acetone and acetone/chloroform for the synthetic reactions and recrystallizations, respectively. Thus, almost all the trinuclear complexes have been successfully synthesized in this one-pot procedure in high yield (70−95%). The μ-$CCl_3CO_2^-$ complex could not be prepared under these conditions. Both the poor σ-electron donor ability of this carboxylate as seen in Taft's substituent parameter[28] (described below) and the bulkiness of CCl_3 can retard the formation of a trinuclear framework. On the other hand, the μ-$(CH_3CH_2)_2CHCO_2^-$ complex (**9**) with a very bulky substituent can be easily synthesized. The inductive effect of the substituent may, therefore, play an important role in the formation of the trinuclear skeletons of the complexes.

Description of the Structures. Selected bond lengths and angles are summarized in Table 1. Perspective views of the monocationic complexes in $\mathbf{1b}\cdot 6H_2O$ and $\mathbf{2b}\cdot 2H_2O$ are shown in Figures 1 and 2, respectively. Overall skeletal structures are very similar to those of other trinuclear chromium(III) carboxylates.[2,3,9,11,18,22] These complexes contain an almost equilateral triangle framework with an oxide ion in the center $[Cr_3O]$. The

---

(25) Otwinowski, Z. *DENZO and SCALEPACK: Computer programs for oscillation data processing*; Mac Science: Tokyo, 1993.

(26) Altomare, A.; Cascarano, G.; Giacovazzo, C.; Guagliardi, A.; Burla, M. C.; Polidori, G.; Camalli, M. *J. Appl. Crystallogr.* **1994**, *27*, 435.

(27) Edwards, C.; Gilmore, C. J.; MaCay, S.; Stewart, N. *CRYSTAN-GM: A computer program for the solution and refinement of crystal structure*; Mac Science: Tokyo, 1996.

(28) Taft, R. W., Jr. In *Steric Effects in Organic Chemistry*; Newman, M. S., Ed.; Wiley: New York, 1956; Chapter 3.

Table 2. Selected Bond Lengths (Å) for Related Trinuclear Carboxylato-Bridged Chromoium(III) Complexes

	Cr−O					
	H_2O	μ_3-O	μ-RCO_2	Cr−Cr	pK_a[a]	ref
$[Cr_3(\mu_3\text{-}O)(\mu\text{-}HCO_2)_6(H_2O)_3]^+$ (**1b**)	2.028(13)	1.909(4)	1.98(1)	3.31(1)	3.75	this work
$[Cr_3(\mu_3\text{-}O)(\mu\text{-}CH_3CO_2)_6(H_2O)_3]^+$ (**2b**)	2.064(18)	1.891(4)	1.97(1)	3.28(1)	4.76	this work
$[Cr_3(\mu_3\text{-}O)(\mu\text{-}CH_2ClCO_2)_6(H_2O)_3]^+$	2.03(2)	1.94(2)	1.98(1)	3.300(6)	2.68	2
$[Cr_3(\mu_3\text{-}O)(\mu\text{-}ValH)_6(H_2O)_3]^{7+}$ [b]	2.03(2)	1.90(1)	2.03(2)	3.30(2)	2.29	10
$[Cr_3(\mu_3\text{-}O)(\mu\text{-}nicH)_6(H_2O)_3]^{7+}$ [c]	2.05(1)	1.906(6)	1.98(1)		4.85	17
$[Cr_3(\mu_3\text{-}O)(\mu\text{-}i\text{-}nicH)_6(H_2O)_3]^{7+}$ [d]	2.046(15)	1.903(3)	1.95(3)			8

[a] Data from: *Critical Stability Constants*; Smith, R. M., Martell, A. E., Eds; Plenum: New York, 1989; Vol. 6. *Merck Index*, 11th ed.; Merck: Rahway, NJ, 1989. [b] valH = L-valine. [c] nicH = nicotinic acid. [d] *i*-nicH = isonicotinic acid.

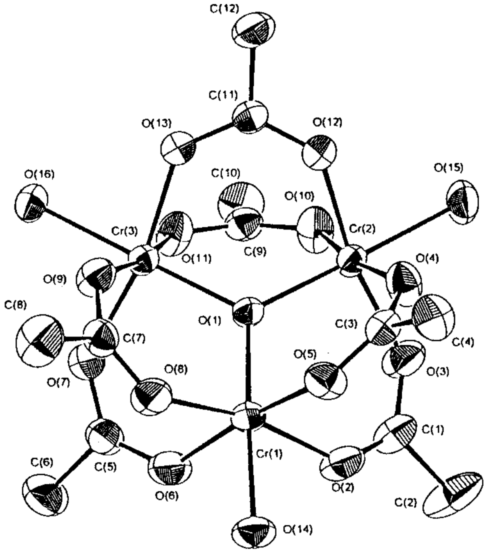

Figure 2. ORTEP drawing of the $[Cr_3(\mu_3\text{-}O)(\mu\text{-}CH_3CO_2)_6(H_2O)_3]^+$ (**2**) cation in the crystals of the $[B(C_6H_5)_4]^-$ salt (**2b**) with the thermal ellipsoids drawn at the 50% probability level.

three chromium(III) ions ($S = {}^3/_2$) in each complex are antiferromagnetically coupled with isotropic coupling constants J of −10.5(1) cm^{-1} (**1b**·$6H_2O$) and −10.9(1) cm^{-1} (**2b**·$2H_2O$), respectively. This indicates that the $[Cr_3O]$ core is equilaterally coupled magnetically in both the complexes.

There is no obvious difference among the Cr−O (in μ-RCO_2) bond lengths in the trinuclear complexes as shown in Table 2; this may be due to the leveling effect by the bridging structure of the carboxylates upon the rigid triangular core of $[Cr_3O]$.

The average $Cr-OH_2$ distances 2.028(13) and 2.064(18) Å for **1b**·$6H_2O$ and **2b**·$2H_2O$, respectively, are significantly longer than those of mononuclear chromium(III) aqua complexes (1.98−2.02 Å).[29] This crystallographic lengthening of $Cr-OH_2$ bonds has been observed with the other chromium(III) trinuclear complexes as shown in Table 2. These structural features correspond to the kinetic behavior where the dissociative mode of the terminal ligand substitution prevails (see below) and seem to be due to a trans influence of the central oxide ion, just as seen in the conjugate base mechanism for the mononuclear complexes.[6] Furthermore, it is found that the $Cr-OH_2$ distance becomes slightly longer with increasing the σ-donating ability in μ-RCO_2^- assessed by the protonation constant, i.e., pK_a of the corresponding carboxylic acid, as shown in Table 2. This substituent effect will be discussed in detail below in connection with the substitution rates.

Preliminary Observations on Substitution Reactions. Although structural characterizations of chromium(III) complexes in solution are usually hampered by the inability to employ ^1H NMR spectroscopy owing to their paramagnetic properties, it was found that ^2H NMR behavior of $CD_3CO_2^-$ coordinated to chromium(III) makes it possible to distinguish among isomers in solution.[30] Attempts were made to obtain changes in ^2H NMR spectra due to the substitution on deuterated $[Cr_3(\mu_3\text{-}O)(\mu\text{-}CD_3CO_2)_6(H_2O)_3]^+$ and $[Cr_3(\mu_3\text{-}O)(\mu\text{-}DCO_2)_6(H_2O)_3]^+$. Both the systems show singlet peaks at δ 40 and 10 (vs TMS), corresponding to the bridging $CD_3CO_2^-$ and DCO_2^- ligands, respectively, and the positions and the intensities of these peaks did not change with time at room temperature in dma. Rather broad line widths of the NMR signals may prevent us from distinguishing among successive substituted species.

Scheme 1

$$[Cr_3(\mu_3\text{-}O)(\mu\text{-}RCO_2)_6(H_2O)_3]^+$$

$$\xrightarrow[-H_2O]{+dma} [Cr_3(\mu_3\text{-}O)(\mu\text{-}RCO_2)_6(dma)(H_2O)_2]^+ \quad k_1$$

$$\xrightarrow[-H_2O]{+dma} [Cr_3(\mu_3\text{-}O)(\mu\text{-}RCO_2)_6(dma)_2(H_2O)]^+ \quad k_2$$

$$\xrightarrow[-H_2O]{+dma} [Cr_3(\mu_3\text{-}O)(\mu\text{-}RCO_2)_6(dma)_3]^+ \quad k_3$$

On the other hand, UV−vis spectra of the trinuclear complexes in dma clearly changed with time (see Figure S1, Supporting Information). The absorption maxima of two d−d bands at ca. 590 and 440 nm shifted to the longer wavelengths (ca. 605 and 455 nm), and their intensities increased, with isosbestic points at 550, 420, and 380 nm. The time course is uniphasic, although there can be three steps in the overall substitution as in Scheme 1.

The final product, $[Cr_3(\mu_3\text{-}O)(\mu\text{-}RCO_2)_6(dma)_3]^+$, was isolated but not in an analytically pure form. The complete replacement of three aqua ligands by the dma ligand was evident from the observation that the ^2H NMR signal of coordinated water at δ ca. 180 of $[Cr_3(\mu_3\text{-}O)(\mu\text{-}RCO_2)_6(D_2O)_3]^+$ in dma decreased with time and finally disappeared.

These results indicate that there are very little differences in the extinction coefficients of visible absorptions among four chromium species ($[Cr_3(\mu_3\text{-}O)(\mu\text{-}RCO_2)_6(H_2O)_3]^+$, $[Cr_3(\mu_3\text{-}O)(\mu\text{-}RCO_2)_6(dma)(H_2O)_2]^+$, $[Cr_3(\mu_3\text{-}O)(\mu\text{-}RCO_2)_6(dma)_2(H_2O)]^+$, and $[Cr_3(\mu_3\text{-}O)(\mu\text{-}RCO_2)_6(dma)_3]^+$) and rates are statistically controlled as claimed by Bourke et al.[1] The absorption band can be clearly assigned to the d−d transition, where the position and the intensity are governed by the environment in the vicinity of the metal center. Both the original triaqua and the final tris(dma) complexes have very similar coordination spheres from the viewpoint of the spectrochemical series situation, and differences in the electronic and steric natures of the Cr−aqua and Cr−dma coordination bonds appear to be slight. Moreover,

---

(29) Brudenell, S. J.; Crimp, S. J.; Higgis, J. K. E.; Moubaraki, B.; Murray, K. S.; Spiccia, L. *Inorg. Chim. Acta* **1996**, *247*, 35.

(30) Fujihara, T.; Abe, Y.; Kaizaki, S. *J. Chem. Soc., Dalton Trans.* **1995**, 1823.

Table 3. Comparison of Kinetic Data for the Ligand Substitution Reactions

complex $[Cr_3(\mu_3\text{-}O)(\mu\text{-}RCOO)_6(H_2O)_3]^+$ R	system	k, s^{-1} (at 25.0 °C)	$\Delta H^‡$, kJ mol^{-1}	$\Delta S^‡$, J K^{-1} mol^{-1}	$\Delta V^‡$, cm^3 mol^{-1}	ref
H (**1**)	$H_2O \rightarrow$ dma	$2.73(2) \times 10^{-5}$	123 ± 2	+81 ± 5	+18.5 ± 0.3	this work
CH_3 (**2**)	$H_2O \rightarrow$ dma	$5.20(1) \times 10^{-4}$	107 ± 2	+51 ± 6	+17.3 ± 0.1	this work
CH_3CH_2 (**3**)	$H_2O \rightarrow$ dma	$6.13(2) \times 10^{-4}$	103 ± 4	+39 ± 13	+12.4 ± 0.2	this work
CH_2Cl (**4**)	$H_2O \rightarrow$ dma	$1.80(4) \times 10^{-5}$	114 ± 2	+47 ± 7	+18.4 ± 0.2	this work
$CHCl_2$ (**5**)	$H_2O \rightarrow$ dma	$1.2(5) \times 10^{-5}$ [a]	121 ± 4	+34 ± 8	+14.4 ± 0.3	this work
CH_3OCH_2 (**6**)	$H_2O \rightarrow$ dma	$2.88(1) \times 10^{-5}$	119 ± 3	+78 ± 11	+21.3 ± 0.3	this work
$(CH_3)_3C$ (**7**)	$H_2O \rightarrow$ dma	$1.35(1) \times 10^{-3}$	99 ± 3	+31 ± 6	+16.7 ± 0.2	this work
CH_2ClCH_2 (**8**)	$H_2O \rightarrow$ dma	$2.89(1) \times 10^{-5}$	108 ± 2	+41 ± 8	+21.0 ± 0.2	this work
$(CH_3CH_2)_2CH$ (**9**)	$H_2O \rightarrow$ dma	$4.13(3) \times 10^{-4}$	98 ± 2	+29 ± 3	+17.4 ± 0.4	this work
$[Cr(H_2O)_6]^{3+}$	H_2O exchange	4.3×10^{-7}	109 ± 1	+1.3 ± 4	−9.3 ± 0.3	35
$[Cr(dmf)_6]^{3+}$ [b]	dmf exchange	5.5×10^{-8}	97.4 ± 2	−43.7 ± 2	−6.3 ± 0.2	36

[a] At 35.0 °C. [b] dmf = *N*,*N*-dimethylformamide.

since there are no direct bonds between Cr centers, the influence of terminal ligands on other Cr centers may be weakened during delivery through three bonds (L−Cr−O−Cr). The additivities in the UV−vis intensities may be due to such a weak metal−metal interaction.

If the weak interaction is also realized for the dynamic behavior, an independence of individual Cr centers in the substitution can be observed. A reasonable hypothesis[1] that the rate of each step is proportional to the number of sites available for substitution (k_1:k_2:k_3 = 3:2:1) may hold, and the first-order relaxation may seem uniphasic up to almost the final stage of the reaction. This is the case in the present systems. Similar behaviors are observed for reactions of analogous trinuclear complexes: the formation and aquation of $[Cr_3(\mu_3\text{-}O)(\mu\text{-}CH_3CO_2)_6(urea)_3]^+$ [1] and the solvolysis of $[Ru_3(\mu_3\text{-}O)(\mu\text{-}CH_3CO_2)_6(H_2O)_3]^+$ and $[Rh_3(\mu_3\text{-}O)(\mu\text{-}CH_3CO_2)_6(H_2O)_3]^+$ in methanol.[6] It was found that the consecutive steps occur with rate constants close to the statistical ratios, suggesting very little cooperative effect between three metal centers.

Kinetic Analysis of the Substitution Reaction. All the systems studied here exhibited very similar kinetic behaviors in the substitution reactions. The intensity of the d−d absorption increased with time. The observed rate constant k_{obs} represents that for the individual Cr center, but not for the whole complex with three Cr centers. Then the substitution rate k is equal to k_{obs}. Tables 3 and S1 (Supporting Information) show the activation parameters and the rates, respectively.

Mechanism of the Substitution Process. The usefulness of the activation volume $\Delta V^‡$ for elucidating the activation mode (associative or dissociative) of inorganic reactions has been reviewed.[31] The sign of $\Delta V^‡$ provides insight into the intimate nature of the activation process. Positive $\Delta V^‡$ values of 12.7−22.1 cm^3 mol^{-1}, as well as large $\Delta H^‡$ and positive $\Delta S^‡$ values, suggest a dissociative activation (I_d or D), which is similar to those for substitutions of terminal ligands of trinuclear ruthenium(III), rhodium(III), and molybdenum complexes as previously reported.[6,12b]

Substituent Effects of Carboxylate Bridging Ligands. The rate constants k varied from $2.4(1) \times 10^{-5}$ to $9.49(2) \times 10^{-3}$ s^{-1} at 40 °C with variation of the carboxylates as summarized in Table S1. To reveal the fundamental details of the substituent effect, we will examine the kinetic data in terms of Taft's equation[28]

$$\log(k/k_0) = \rho^*\sigma^* + \delta E_s$$

where σ^* and E_s are the inductive and steric constants for an aliphatic substituent, respectively.[28] The parameters ρ^* and δ remain constant through a class of reactions and are independent of the nature of the substituent groups. The quotient k/k_0 is the relative rate for any substituent of the μ-carboxylate ligands, where k_0 is the rate constant for the standard reactant (in the present case the $\mu\text{-}CH_3CO_2^-$ complex (**2**)). Application of the equation to the present series including nine trinuclear complexes gave the parameters $\rho^* = 1.17$ and $\delta = 0$ with a correlation coefficient of 0.972 as shown in Figure 3. These results indicate that the substitution rate for the terminal aqua ligand is influenced only by the electronic properties, i.e., σ-donating ability, not by the steric factors of the bridging carboxylate ligand.

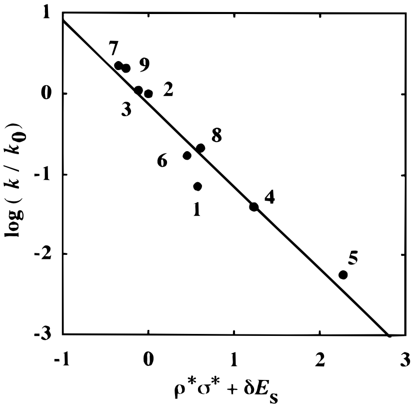

Figure 3. Taft relationship of the rate constant of dimethylacetamide (dma) substitution for aqua ligands of $[Cr_3(\mu_3\text{-}O)(\mu\text{-}RCO_2)_6(H_2O)_3]^+$ in dma: $\log(k/k_0)$ vs $\rho^*\sigma^* + \delta E_s$ (see text). R = H (**1**), CH_3 (**2**), CH_3CH_2 (**3**), CH_2Cl (**4**), $CHCl_2$ (**5**), CH_3OCH_2 (**6**), $(CH_3)_3C$ (**7**), CH_2ClCH_2 (**8**), and $(CH_3CH_2)_2CH$ (**9**).

The static cis electronic influence of the bridging carboxylate on the $Cr-OH_2$ bond have been observed in the present system: the difference in the $Cr-OH_2$ bond distances between $\mu\text{-}HCO_2^-$ (**1b**) and $\mu\text{-}CH_3CO_2^-$ complexes (**2b**). This may arise from the cooperative charge redistribution due to the electroneutrality principle in a complex as a whole, as found for the spectroscopic and structural behavior for the *trans*- and *cis*-$[MX_2(N)_4]$ types of chromium(III), cobalt(III), and nickel(II) complexes with various kinds of amines.[32−34] For the chromium(III) complexes, Kaizaki and co-workers precisely elucidated the cis effect using angular overlap model (AOM) parameters in their studies of the solvent-dependent ^2H NMR spectra and solvatochromism in ligand field absorption bands in various organic solvents.[32,33] The σ-bonding interactions of the equatorial ligands influence those of the axial ones. In the

---

(31) van Eldik, R.; Asano, T.; le Noble, W. J. *Chem. Rev.* **1989**, *89*, 549.

(32) Terasaki, Y.; Kaizaki, S. *J. Chem. Soc., Dalton Trans.* **1995**, 2837.

(33) Kaizaki, S.; Takemoto, H. *Inorg. Chem.* **1990**, *29*, 4960.

present system, only the σ-donor ability of the bridging carboxylate seems to be due to the static cis effect and the σ-bonding of Cr−OH$_2$ becomes weaker, simply when the bridging carboxylate is much stronger as a σ-donor.

The rate constants for the trinuclear complexes are compared with those of the solvent exchange reactions of the mononuclear chromium(III) complexes[35,36] in Table 3. The first-order rate constant of the dma substitution for the aqua ligand in the μ-$(CH_3)_3CCO_2^-$ complex (**7**) is more than 2.4×10^4 times larger than that of the bulk solvent exchange of $[Cr(dmf)_6]^{3+}$ (dmf = dimethylformamide).[36] The difference is less remarkable in the case of the μ-$CHCl_2CO_2^-$ complex (**5**) even at 35 °C, but ca. 200 times acceleration was observed. The Cr−OH$_2$ distances are significantly longer than those of the mononuclear chromium(III) aqua complexes as described in the previous section. The static weakening of Cr−O bonds in the trinuclear complexes plays a role in accelerating the terminal substitution, since it proceeds exclusively via a dissociative mechanism, where the leaving of the bound ligand determines the rate. Such kinetic trans and cis mutual interactions are common dynamic features of the terminal sites in the present μ_3-oxo−μ-carboxylate-bridged trinuclear complexes.

Supporting Information Available: A table showing the reaction rates (Table S1) and figures showing changes in absorption spectra (Figure S1) and changes in absorbance (Figure S2) (5 pages). X-ray crystallographic files for **1b**·6H$_2$O and **2b**·2H$_2$O, in CIF format, are available on the Internet only. Ordering and access information is given on any current masthead page.

IC980001G

---

(34) (a) Martin, L. Y.; Sperati, C. R.; Busch, D. H. *J. Am. Chem. Soc.* **1977**, *99*, 2968. (b) Hung, Y.; Martin, L. Y.; Jackels, S. C.; Tait, A. M.; Busch, D. H. *J. Am. Chem.* Soc. **1977**, *99*, 4030. (c) Ito, T.; Kato, M.; Ito, H. *Bull. Chem. Soc. Jpn.* **1984**, *57*, 1556. (d) Ito, T.; Kato, M.; Ito, H. *Bull. Chem. Soc. Jpn.* **1984**, *57*, 2641. (e) Bertini, I.; Gatteschi, D.; Scozzafava, A. *Inorg. Chem.* **1976**, *15*, 203. (f) Lever, A. B. P.; Walker, I. M.; MacCarthy, P. J.; Mertes, K. B.; Jircitano, A.; Scheldon, R. *Inorg. Chem.* **1983**, *22*, 2252. (g) Deeth, R. J.; Gerloch, M. *Inorg. Chem.* **1987**, *26*, 2582. (h) Deeth, R. J.; Gerloch, M. *Inorg. Chem.* **1984**, *23*, 3846.

(35) Stranks, D. R.; Swaddle, T. W. *J. Am. Chem. Soc.* **1971**, *93*, 2783.

(36) Lo, S. T. D.; Swaddle, T. W. *Inorg. Chem.* **1975**, *14*, 1878; **1976**, *15*, 1881.